^{1}H NMR Spectroscopic Studies of Calcium-Binding Proteins. 3. Solution Conformations of Rat Apo-α-parvalbumin and Metal-Bound Rat α-Parvalbumin†

Thomas C. Williams,* David C. Corson, Kimio Oikawa, William D. McCubbin, Cyril M. Kay, and Brian D. Sykes
Medical Research Council of Canada Group in Protein Structure and Function and Department of Biochemistry, University of Alberta, Edmonton, Alberta, Canada T6G 2H7

Received July 18, 1985

ABSTRACT: Lacking the extraordinary thermal stability of its metal-bound forms, apo-α-parvalbumin from rat muscle assumes *two* distinct conformations in aqueous solution. At 25 °C, its highly structured form predominates (K_{eq} = 5.7; $\Delta G°$ = −4.3 kJ·mol^{-1}); as deduced from both ^{1}H NMR and circular dichroism (CD) spectroscopy, this conformation is exceedingly similar to those of its Mg(II)-, Ca(II)-, and Lu(III)-bound forms. The temperature dependences of several well-resolved aromatic and upfield-shifted methyl ^{1}H NMR resonances and several CD bands indicate that the native, highly helical structure of rat apo-α-parvalbumin is unfolded by a concerted mechanism, showing no indication of partially structured intermediates. The melting temperature, T_M, of rat apo-α-parvalbumin is 35 ± 0.5 °C as calculated by both spectroscopic techniques. By 45 °C, rat apo-α-parvalbumin unfolds entirely, losing the tertiary structure that characterizes its folded form: not only are the ring-current-shifted aromatic and methyl ^{1}H NMR resonances leveled, but the 262- and 269-nm CD bands are also severely reduced. As judged by the decrease in the negative ellipticity of the 222-nm CD band, this less-structured form of rat apo-α-parvalbumin shows an approximate 50% loss in apparent α-helical content compared to its folded state. Several changes in the ^{1}H NMR spectrum of rat apo-α-parvalbumin were exceptionally informative probes of the specific conformational changes that accompany metal ion binding and metal ion exchange. In particular, the line intensities of the ortho proton resonance of Phe-47, the unassigned downfield-shifted α-CH resonances from the β-sheet contacts between the metal-binding loops, the C_2H resonance of His-48, and the ϵ-CH_3 resonance of an unassigned Met residue were monitored as a function of added metal to determine the stability constants of several metal ion–parvalbumin complexes. We conclude that Mg(II) binds to the CD and EF sites independently, its affinity for the EF site being almost twice that for the CD site. Mg(II) → Ca(II) exchange showed that the CD-site Mg(II) is displaced first, in contrast to Lu(III)'s preferential displacement of the EF-site Ca(II) as determined from the Ca(II) → Lu(III) exchange experiments. The stability constants, β, so determined are as follows: $\beta_{Mg:CD} = 5.6 \times 10^4$ M^{-1}; $\beta_{Mg:EF} = 8.3 \times 10^4$ M^{-1}; $\beta_{Ca:CD} = 1.7 \times 10^8$ M^{-1}; $\beta_{Ca:EF} = 9.1 \times 10^7$ M^{-1}; $\beta_{Lu:CD} = 2.0 \times 10^{10}$ M^{-1}; $\beta_{Lu:EF} = 2.3 \times 10^{11}$ M^{-1}. We suggest that the increases in the negative ellipticity of the 222-nm CD band that accompany Mg(II) and Ca(II) chelation (5 and 13%, respectively) arise not from an increase in α-helical content but rather from the ordering of carbonyl-containing ligands at the CD- and EF-binding sites. Furthermore, we suggest that the extraordinary thermal stabilities of the divalent and trivalent metal ion forms of parvalbumin arise primarily from the efficient reduction of the charge–charge repulsions of the anionic chelating groups. This description of parvalbumin's structure and metal ion exchange properties agrees well with its proposed functions as the soluble relaxation factor in contractile systems and as a Ca(II) buffer in nonmuscle systems [Pechère, J.-F., Derancourt, J., & Haiech, J. (1977) *FEBS Lett.* *75*, 111–114].

Complex formation between metal ions and multidentate ligands is governed primarily by an entropic process: the *chelate effect* (Schwarzenbach, 1952; Cotton & Harris, 1956; Beck, 1970). Diffusional freedom of one coordinating group from another in a multidentate ligand is limited by the covalent bonds that join them. Formation of a ligand–metal bond by one group dramatically enhances the effective concentration of the others, restricting their spatial freedom to the immediate vicinity of the metal. If the network of covalent bonds permits, these restricted liganding groups are statistically favored to coordinate the first-bound metal ion. From linear bidentates to branched multidentate ligands to chelate cages (i.e., cryptands), the progressive increase in the stabilities[1] of different complexes of a given metal ion correlates well with the degree to which the chelating groups are restricted by the inherent structure of the ligand and the ionic size of the metal. This dependence of the stability of a complex on ligand restriction is exemplified extraordinarily well by a class of biochemical chelators known as calcium-binding proteins. As determined from the crystal structure of one such protein, carp parvalbumin pI = 4.25 (Kretsinger & Nockolds, 1973), each bound Ca(II) is fixed within an octahedral-like cage of oxygen ligands formed by the inward projections of alternating residues in a 12-residue loop that encircles the metal ion. In native proteins, this Ca(II)-binding loop constitutes only part of a larger functional domain. From each end of the loop extends a section of α-helix approximately three turns long. These

† This work was supported by the Medical Research Council of Canada Group in Protein Structure and Function and the Alberta Heritage Foundation for Medical Research (equipment grant for the NT-300WB spectrometer and fellowship and research allowance to T.C.W.).

[1] In accordance with the standard convention of expressing metal ion complex equilibria as formation reactions (IUPAC Comission on Equilibrium Data, 1979), the metal complexes of parvalbumin are described here in terms of their overall stability constants, β, rather than as dissociation constants, K_d, as has been done frequently in the past. Stability constants referred to in this work are identified by a double index: the first subscript indicates the type of metal ion bound and the second specifies which site in parvalbumin is involved in chelation.

0006-2960/86/0425-1835$01.50/0

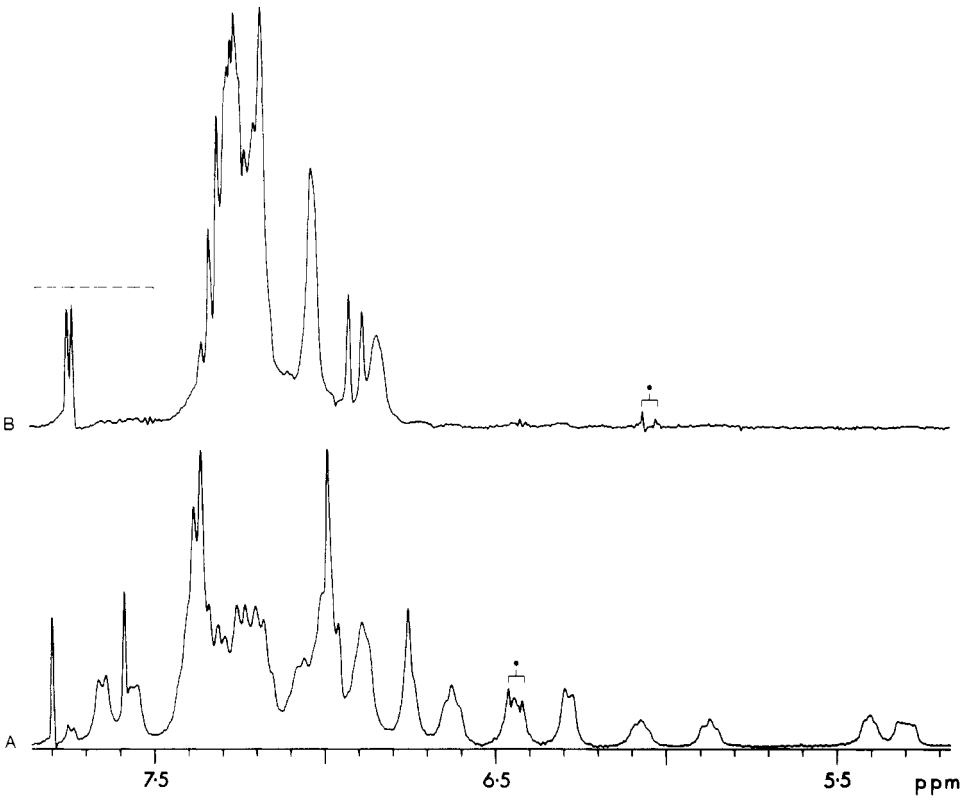

FIGURE 1: Aromatic region (7.9–5.2 ppm) of the 300-MHz ^{1}H NMR spectrum of rat apoparvalbumin. Sample conditions: 150 mM KCl/10 mM piperazine, pH 7.5 (in D_2O). (A) 25 °C; (B) 45 °C. The region delimited by the dashed bracket is plotted as a function of temperature in Figure 5. The doublet-like peaks denoted by (●) at 6.44 ppm in spectrum A and at 6.07 ppm in spectrum B are spectral artifacts; a triplet meta proton Phe resonance is beneath this artifact in spectrum A.

helix–loop–helix domains are never found as isolated units within native proteins, occurring instead as paired helix–loop–helix domains or, as in the case of parvalbumins, as a triad of helix–loop–helix domains. The loop itself binds Ca(II) ions only weakly, the stability constant of a synthetic 13-residue analogue being in the order of 10^2 M^{-1} (Gariepy et al., 1983). Given the size of the chelate rings formed by such ligands (i.e., $\overline{X–O–Ca–O}$; where X ~ 10 atoms), this is not surprising. Larger analogues of helix–loop–helix domains that incorporate both N- and C-terminal helical sections have greater Ca(II) complex stability constants, being about 10^4–10^5 M^{-1} for synthetic 26–34-residue peptides (Reid et al., 1981; Gariepy et al., 1982), 10^5 M^{-1} for the cyanogen bromide cleavage fragment 9 of troponin C (site III), and 10^4 M^{-1} for the thrombin digest fragment 2 of troponin C (site IV; Leavis et al., 1977). The stability constants of paired domains such as found in calmodulins and troponin C's range from 10^5 to 10^7 M^{-1} (Potter & Gergely, 1975; Haiech et al., 1981). Parvalbumins, although their N-terminal domain fails to bind Ca(II), possess the strongest stability constants of any protein in this class: each of their two functional sites binds Ca(II) with an affinity of about 10^8 M^{-1} (Haiech et al., 1979). However, pike III parvalbumin, when selectively cleaved by cyanogen bromide to remove its defunct N-terminal domain, suffers a severe loss in Ca(II)-binding capacity, its stability constants falling to 10^5 M^{-1} (Maximov & Mitin, 1979). The unusually high affinities of parvalbumins for calcium and an apparent lack of protein–protein interactions are believed to reflect their physiological role as a Ca(II) buffer (Pechere et al., 1977). In the resting state, the [Ca(II)] within myofibrils is extremely low ($<10^{-7}$ M), and parvalbumin is presumed to exist in solution as a noninteracting Mg(II)-loaded protein. Stimulated influx of extracellular Ca(II) initially saturates the Ca(II)-specific sites of troponin C, followed by competitive exchange of Ca(II) into Mg(II)-filled protein sites. The translocation of Ca(II) from its functionally significant troponin C binding sites to the cell exterior is believed to be facilitated by its binding to the CD[2] and EF sites of parvalbumin prior to its sequestration in the sarcoplasm. The metal ion exchange characteristics of parvalbumin have been likened to the exchange characteristics of the extremely efficient and structurally rigid chelators called cryptands (Williams et al., 1984). To further test parvalbumin's apparent similarity to cryptands, we have used ^{1}H NMR and CD spectroscopy to study in detail the structural changes induced by metal ion binding to rat apo-α-parvalbumin and by metal ion exchange in several of its metal-bound forms.

Experimental Procedures

Materials. The α-lineage isoform of parvalbumin was isolated from Sprague-Dawley rats by the method of Haiech et al. (1979); its purity was verified by amino acid analysis (Berchtold et al., 1982), UV absorption and ^{1}H NMR spectroscopy, and SDS–polyacrylamide gel electrophoresis. Chelex-100 (50–100 mesh) and D_2O (99.8 mol %) were purchased from Bio-Rad Corp. Xylenol orange was purchased from Terochem Laboratories. KCl, $MgCl_2$, $CaCl_2$ (puratronic grade; metals basis), and lutetium chloride ($LuCl_3 \cdot cH_2O$; REO purity) were purchased from Alpha Inorganics, Ventron Division.

Preparation of Apo-α-parvalbumin. Rat parvalbumin was decalcified by a variation of the heated-Chelex method (Bose & Bothner-By, 1983): 50 mg of salt-free protein was dissolved

[2] Abbreviations: AB, helix A–loop–helix B region of parvalbumin (residues 7–34); CD, helix C–loop–helix D region of parvalbumin (residues 39–71); EF, helix E–loop–helix F region of parvalbumin (residues 78–108); NMR, nuclear magnetic resonance; CD, circular dichroism; UV, ultraviolet; EDTA, ethylenediaminetetraacetic acid; SDS, sodium dodecyl sulfate; D_2O, deuterium oxide; Pipes, 1,4-piperazinediethanesulfonic acid; DSS, sodium 4,4-dimethyl-4-silapentane-1-sulfonate.

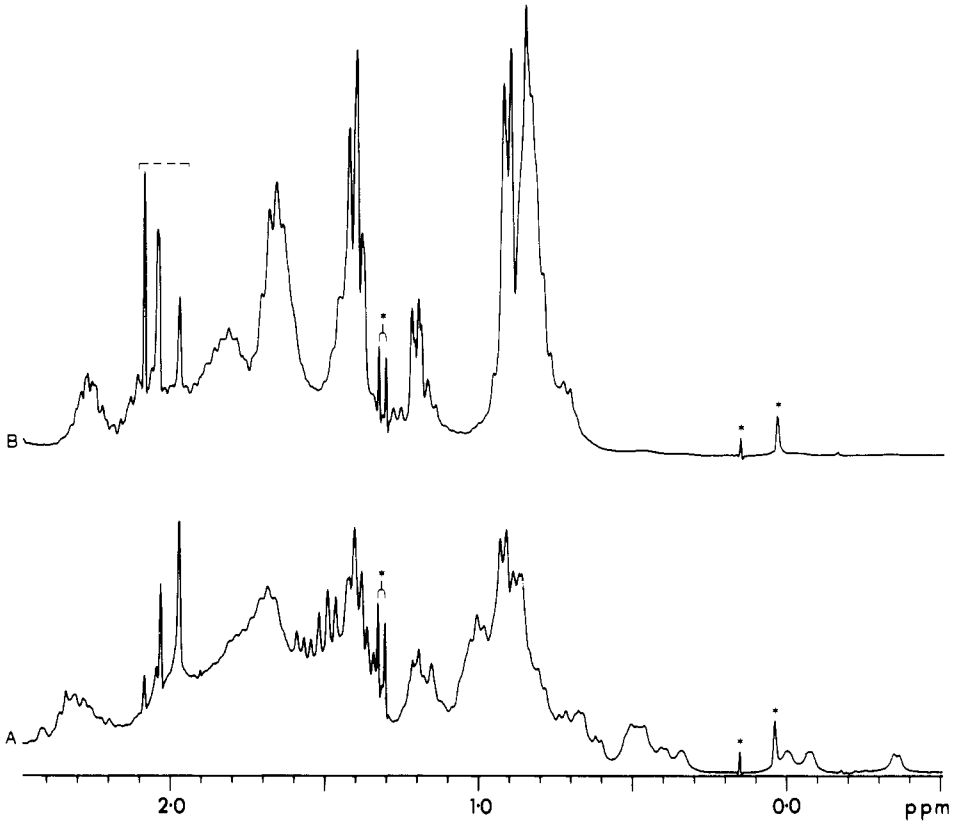

FIGURE 2: Aliphatic region (2.5 to −0.5 ppm) of the 300-MHz ^{1}H NMR spectrum of rat apoparvalbumin. Sample conditions are the same as for Figure 1. (A) 25 °C; (B) 45 °C. The region delimited by the dashed bracket is plotted as a function of temperature in Figure 5. The resonances denoted by (*) are impurities: the doublet resonance at 1.32 ppm and the singlet resonance at 0.151 ppm are derived from contaminants frequently introduced into the sample from the D_2O; the singlet resonance at 0.03 ppm is derived from a contaminant introduced into the sample by the heated-Chelex decalcification method.

in 5.0 mL of 15 mM KCl/1 mM piperazine, pH 9.0, introduced into a drained, preequilibrated resin bed of Chelex 100, heated to 60 °C for 45 min, eluted from the column directly into an acid-washed Teflon bottle, and then immediately lyophilized. Residual Ca(II) content of this protein sample was estimated as <0.1 mol/mol of parvalbumin from atomic absorption analyses. Protein concentrations were determined from amino acid analyses of 10-μL aliquots.

Preparation of Metal(II) and Metal(III) Solutions. Mg(II) and Ca(II) stock stolutions were prepared from their chloride salts. Samples of each (10–20 mg of their hydrated salts) were dissolved separately in 2.0 mL of D_2O, acidified with DCl to effect total dissolution, and lyophilized. After the dissolution/lyophilization steps were repeated once more, the dried samples were dissolved in final aliquots of D_2O (2.0 mL). Their metal(II) ion concentrations were determined by flame atomic absorption spectroscopy. The Lu(III) stock solution was prepared and standardized following published procedures (Corson et al., 1983a).

^{1}H NMR Spectroscopic Methods. High-resolution 300-MHz ^{1}H NMR spectra of parvalbumin were acquired on a Nicolet Instruments NT-300WB spectrometer. Typical acquisition parameters were as follows: probe size = 5 mm; protein concentration = 2–5 mM; sample volume = 500 μL; spectral width = ±2000 Hz/16K data points; pulse length = 8 μs; preacquisition delay = 100 μs; free induction decay filter = Bessel (±3000 Hz) with quadrature phase detection; number of acquisitions = 1000; resolution enhancement = Lorentzian to Gaussian. Salt-free Ca(II)-bound parvalbumin samples were dissolved in 150 mM KCl/D_2O at 23 °C, lyophilized once to reduce the residual HDO content, and then redissolved in the same volume of unsalted D_2O. Samples of rat apo-α-parvalbumin, prepared by the heated-Chelex method described above, contained both KCl and piperazine; they were twice dissolved in and once lyophilized from sufficient D_2O to reduce HDO and to ensure adequate ionic strength (100–200 mM KCl equivalent). Mg(II)–parvalbumin, generated from the titration of its apo form at 25 °C, was titrated directly with Ca(II) at 45 °C; Ca(II)–parvalbumin, isolated by the methods described above, contained neither excess Ca(II) nor Mg(II) and was titrated with Lu(III) at 40 °C with the methods described by Corson et al. (1983b). All chemical shifts were referenced to the singlet resonance at 0.151 ppm (relative to DSS) of an unidentified impurity in the solvent.

CD Spectroscopic Methods. The CD measurements were made on a Jasco J-500C spectropolarimeter with a DP 500N data processor, equipped with a thermostated cell holder. The instrument was calibrated with an aqueous solution of *d*-10-camphorsulfonic acid (Eastman Organic Chemicals, recrystallized) at 290 and 192.5 nm and checked with an aqueous solution of D(−)-pantoyllactone at 220 nm. The near-UV CD measurements were made in a special 1-cm cell (0.6-mL volume), and the far-UV studies were effected in 0.5-mm cells. The temperature inside the cells was calibrated with a Fluke multimeter with an 80 T150 temperature accessory. The mean residue molecular ellipticities were calculated in accordance with procedures elaborated by Oikawa et al. (1968), with a mean residue weight for rat α-parvalbumin of 106.

RESULTS

Portions of the 300-MHz ^{1}H NMR spectrum of apo-α-parvalbumin from rat skeletal muscle are shown in Figures 1 and 2. At 25 °C, both the aromatic region (Figure 1A)

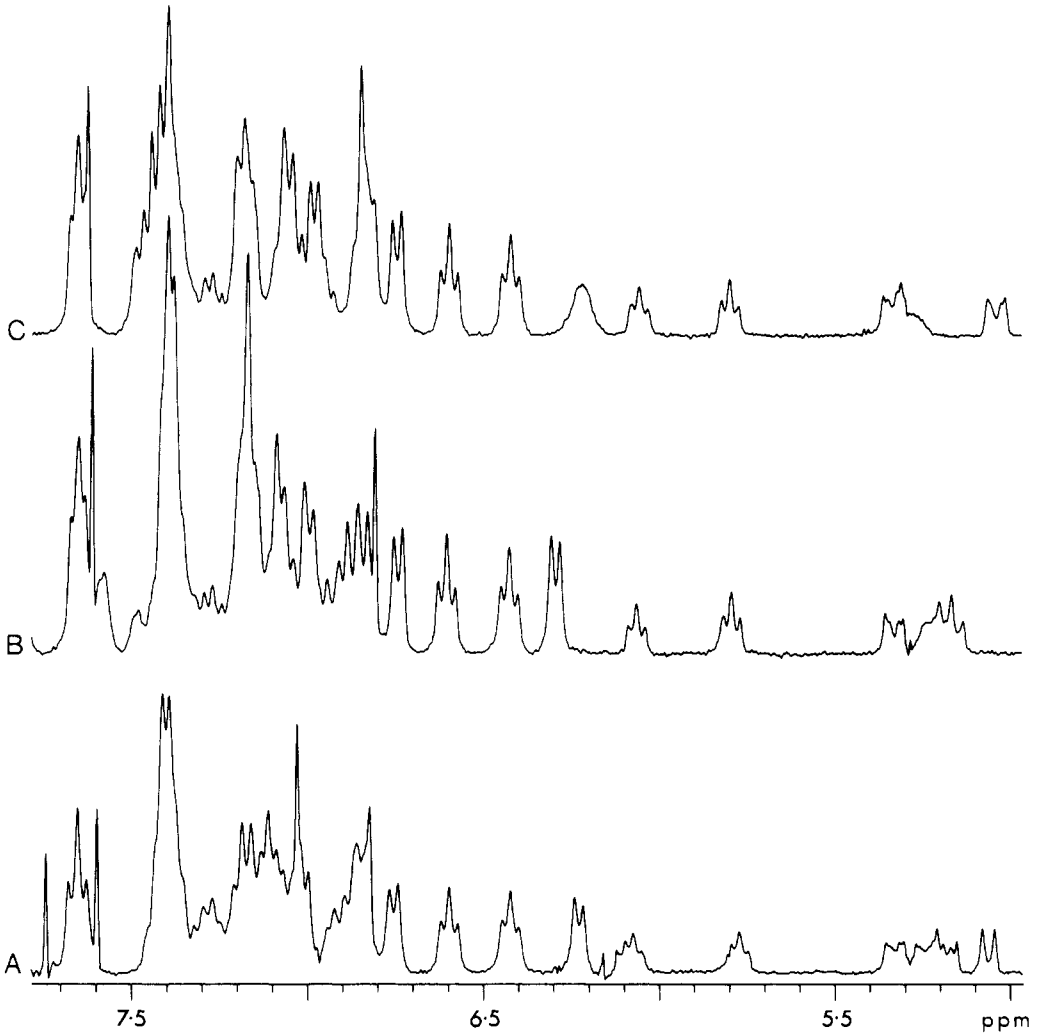

FIGURE 3: Comparison of the aromatic region (7.8–5.0 ppm) of the ^{1}H NMR spectra of three metal-bound forms of rat parvalbumin at 40 °C: (A) Mg(II)–parvalbumin (2.5 mM, 150 mM KCl, 10 mM piperazine, pH 7.7); (B) Ca(II)–parvalbumin (3.5 mM, 150 mM KCl, pH 6.8); (C) Lu(III)–parvalbumin (3.5 mM, 150 mM KCl, pH 6.8).

and the aliphatic region (Figure 2A) showed indications of extensive tertiary structure: most of the upfield-shifted phenylalanine ring proton resonances (7.0–5.8 ppm) and upfield-shifted methyl proton resonances (2.0 to −0.5 ppm) deviate very little, if at all, from their positions in the metal-bound forms (Figures 3 and 4). Both near- and far-UV regions of the CD spectra of the apo and metal-bound forms corroborated this similarity in their structures of 25 °C; relative to the negative ellipticity of the 222-nm band in Mg(II)–parvalbumin, the ellipticity of the 222-nm band in the apo form was 0.88 whereas the ellipticity for the Ca(II) form was 1.09 (Figure 6A) and relative to the average negative ellipticities of the 262- and 269-nm bands in Mg(II)–parvalbumin, the ellipticity of the apo form was again 0.88 whereas the ellipticity of Ca(III)–parvalbumin was 1.12 (Figure 7). These monitors of both secondary and tertiary structures indicated that at 25 °C rat apo-α-parvalbumin is very similar to its metal-bound forms. As indicated by its ^{1}H NMR spectrum in Figure 1A, there was also a second form of rat apo-α-parvalbumin present at 25 °C. The small, doublet-like resonance at 7.75 ppm corresponded to a 15% proportion of this second form, more clearly illustrated at 45 °C (Figure 1B). This "doublet" arose from the overlap of the histidine C_2H resonances of parvalbumin's less-structured form (see below). This taken into account, the negative ellipticities of the 222- and 262/269-nm bands for the folded form of rat apo-α-parvalbumin at 25 °C were adjusted to 0.96 and 0.94, respectively, relative to the Mg(II) form (assuming inherent negative ellipticities of these bands of only 0.4 times those of the more-structured forms as determined from the ellipticities at 45 °C; see Figures 6A and 7A).

Thermal Stability Studies. (*A*) *Apo-α-parvalbumin.* When heated to 45 °C, rat apo-α-parvalbumin lost all of those ^{1}H NMR spectral features that characterized its native tertiary fold (Figures 1B and 2B): most of the aromatic resonances coalesced into a poorly resolved band at 7.3 ppm, and the C_2H and C_5H proton resonances of the two histidines[3] assumed nearly identical chemical shifts (at 7.76/7.74 and 6.93/6.90 ppm, respectively). In addition, the two clearly resolved α-CH resonances at 5.4 and 5.3 ppm in Figure 1A were lost upon heating above 45 °C. The spread of methyl proton resonances also collapsed into discrete bands centered at 0.9, 1.4 and 1.7 ppm. The thermal denaturation of the highly structured form of rat apo-α-parvalbumin was more fully characterized over the 25 → 45 °C temperature range. As shown in Figure 5, the C_2H proton resonances of His-26 and His-48 in the folded form (7.59 and 7.80 ppm, respectively) steadily decreased in intensity until, at 45 °C, they dissappeared. Likewise, two sets of unassigned ortho Phe doublet resonances (7.65 and 7.56

[3] In accordance with nomenclature recommendations (IUPAC-IUB Joint Commission on Biochemical Nomenclature, 1985), we refer to the imidazole ring protons as C_2H and C_5H rather than C_2H and C_4H as has been done frequently in the past.

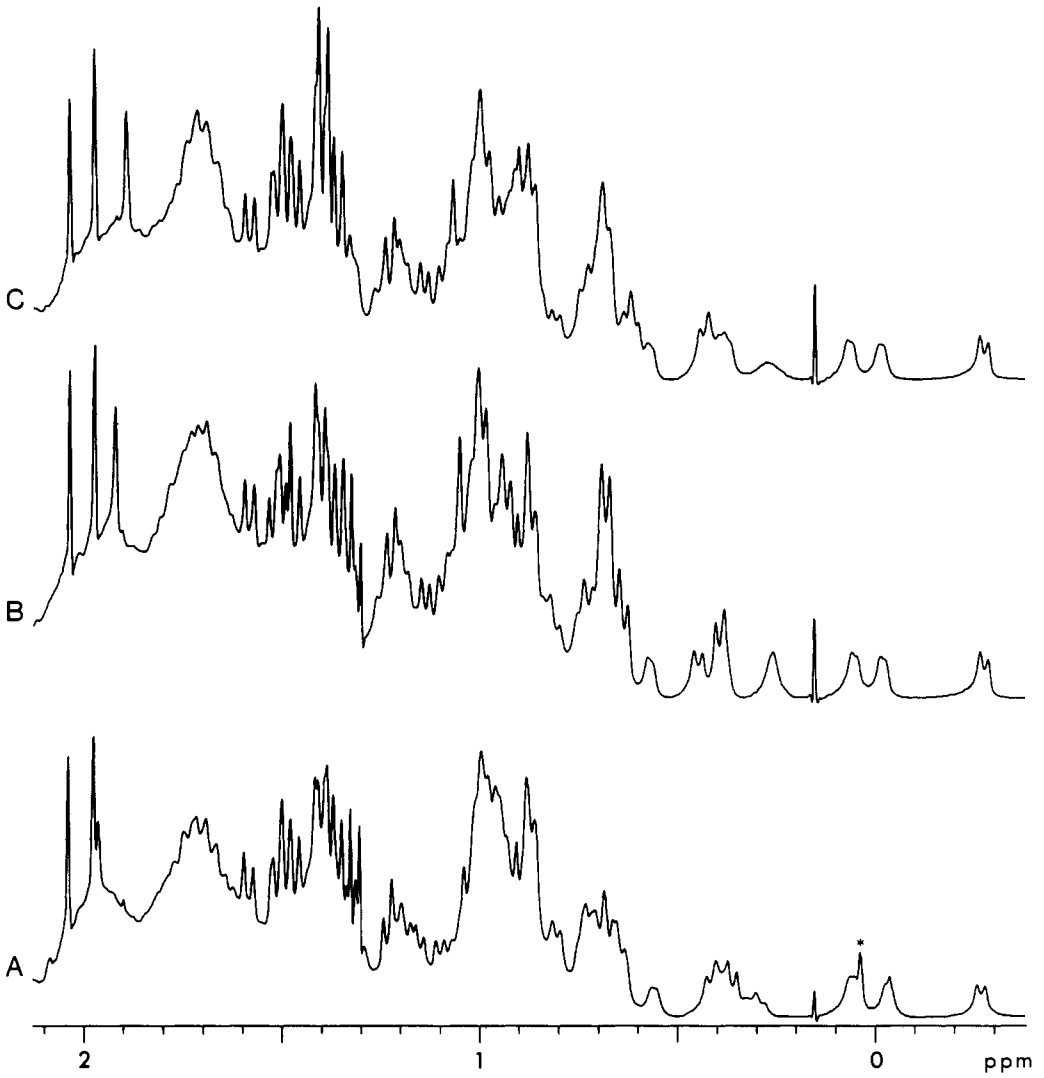

FIGURE 4: Comparison of the aliphatic region (2.5 to −0.5 ppm) of the ^1H NMR spectra of three metal-bound forms of rat parvalbumin at 40 °C: (A) Mg(II)–parvalbumin (2.5 mM, 150 mM KCl, 10 mM piperazine, pH 7.7); (B) Ca(II)–parvalbumin (3.5 mM, 150 mM KCl, pH 6.8); (C) Lu(III)–parvalbumin (3.5 mM, 150 mM KCl, pH 6.8).

ppm) were gradually reduced to zero by this increase in temperature. Conversely, the two closely spaced singlet resonances at 7.75 and 7.74 ppm grew in intensity as the temperature was raised, reaching a maximum at 45 °C. Changes of this type are characteristic of slow exchange between two conformationally different forms. From curve analyses of each resonance in each spectrum of this series, the relative amounts of unfolded and folded forms of rat apo-α-parvalbumin were determined.

The right-hand side of Figure 5 shows a similar series of changes in the *N*-acetyl/methionine ε-CH_3 region of the ^1H NMR spectrum. The singlet resonance at 2.03 ppm, assigned to the *N*-acetyl methyl protons of the folded form, decreased in intensity as the temperature was increased, falling to near zero at 45 °C. However, the apparent singlet at 1.97 ppm, attributed to two coincidentally overlapping Met ε-CH_3 groups, showed only a moderate decrease in intensity. The resonance at 1.97 ppm in the 45 °C spectrum was assumed to be one of four singlet resonances (at 2.09, 2.05, 2.04, and 1.97 ppm), attributed to the *N*-acetyl group and three Met ε-CH_3's of the unfolded form, which increased in intensity as the temperature was raised. Neglecting loss of resonance intensity due to H → D exchange at the imidazole C_2 position, we determined the areas of these resonances as a function of temperature, normalized to the sum of the four singlet C_2H resonances at 7.80, 7.75, 7.74, and 7.59 ppm. The intensities of the resonances at −0.35 (Val-106), 6.29 (Phe-47), 6.62 (Phe-24), 6.07, 5.87, 5.41, and 5.30 ppm were also monitored during the temperature increase; together with the changes illustrated in Figure 5, these defined a single melting profile of the tertiary structure of rat apo-α-parvalbumin (Figure 6B). Because the ratio of the sum of the 7.80 and 7.59 ppm resonances to the sum of all for singlet resonances was 0.85 (Figure 5, left-hand side, 25 °C), the initial relative intensities of all other monitored resonances was taken as 0.85. The temperature-induced reductions in the negative ellipticities of the 262- and 269-nm CD bands (Figure 7A) corroborated the NMR-deduced loss of tertiary structure during transition from the folded to the unfolded form.

The thermal denaturation of rat apo-α-parvalbumin's secondary structure was monitored by the gradual decrease in the negative ellipticity of the 222-nm CD band. As shown in Figure 6A, the normalized ellipticity (i.e., the ratio of the ellipticity at a given temperature to the ellipticity of the apo form at its minimum temperature, 7 °C) followed a sigmoidal decline in intensity, decreasing to an ellipticity at 60 °C of only 0.4 times that at 7 °C. Equilibrium constants for the formation of the folded form of rat apo-α-parvalbumin were calculated from both the NMR and CD data. To evaluate ΔH_d for this denaturation reaction, $\ln K_{eq}$ was plotted vs. $-1/T$

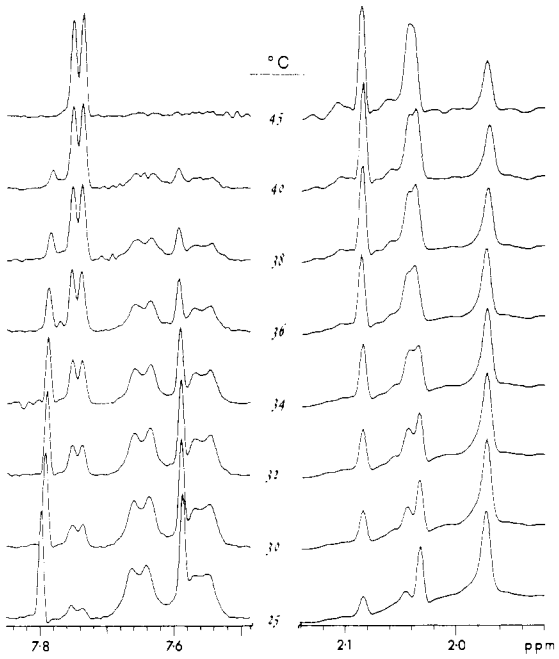

FIGURE 5: Temperature dependence of two regions of the ^{1}H NMR spectrum of rat apoparvalbumin. The left-hand stacked plot illustrates the changes in the His C_2H spectral region; the right-hand stacked plot illustrates the changes in the *N*-acetyl/methionine ϵ-CH_3 spectral region. Acquisition temperatures were as indicated.

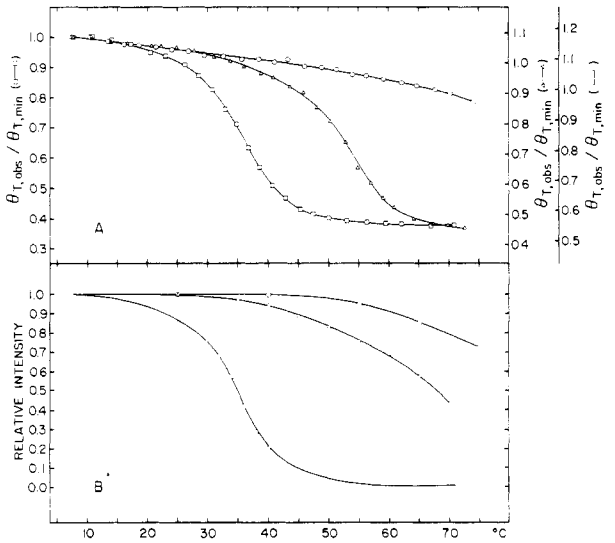

FIGURE 6: Thermal denaturation of rat parvalbumin. (A) Determined from the ellipticity of the 222-nm CD band relative to the apo form at 7.7 °C (sample conditions: 200 mM KCl, 10 mM piperazine, pH 7.74): apoparvalbumin (□); Mg(II)–parvalbumin (△); Ca(II)–parvalbumin (○). The [θ] scales for the metal-bound forms have been shifted to normalize their maximum value at the low-temperature extreme. (B) Determined from changes in the relative intensities of selected ^{1}H NMR resonances (see text; sample conditions same as in Figure 1): apoparvalbumin (□); Mg(II)–parvalbumin (△); Ca-(II)–parvalbumin (○).

according to the van't Hoff temperature dependence of ln K_{eq}. The NMR and CD data defined a single sigmoid function over the 20–60 °C range, the minimum K_{eq} for this cooperative denaturation reaction presumably being below 7 °C (Tanford, 1968). This nonlinearity is an indication that ΔH_d is itself temperature dependent. A first approximation of ΔH_d was calculated from the linear slope of a least-squares fit of the 30–40 °C range. The enthalpy change ΔH = 183 kJ·mol^{-1} (43 kcal·mol^{-1}), combined with ΔG = 2.9 kJ·mol^{-1} (0.7 kcal^{-1}) at 30 °C yielded a calculated ΔS of 0.59 kJ·deg^{-1} mol^{-1} (142 cal·deg^{-1}·mol^{-1}). The melting temperature of rat apo-α-par-

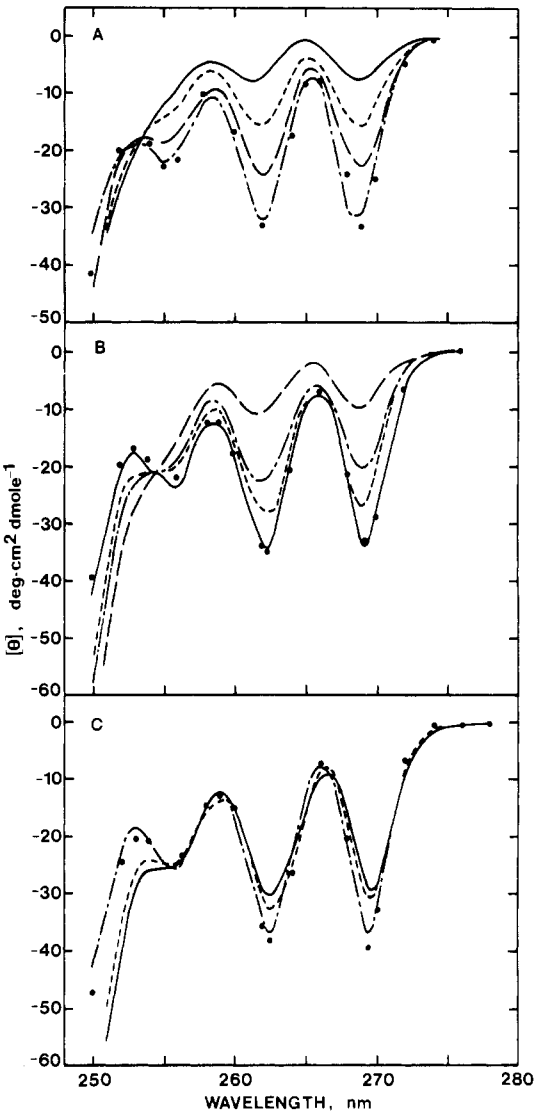

FIGURE 7: Temperature dependence of the near-UV CD spectra of three forms of rat parvalbumin (200 mM KCl, 10 mM piperazine, pH 7.74): (A) apo form at 4.9 (---), 30.2 (--), 36.0 (---), and 46.5 °C ( ); (B) Mg(II) form at 7.0 (—), 47.1 (---), 55.6 (--), and 63.1 °C (--); (C) Ca(II) form at 6.5 (--), 53.4 (---), and 66.9 °C (—). The solid circles indicate the ellipticities of the recooled samples at the specified wavelengths.

valbumin's secondary structure calculated from the decrease in ellipticity at 222 nm (T_M = 35 °C) was identical with the T_M calculated from the changes in the ^{1}H NMR resonance intensities (Figure 6B). This result is very similar to the T_M = 32 °C determined for carp p*I* = 4.25 apoparvalbumin (Filimonov et al., 1978).

(B) Mg(II)- and Ca(II)-Parvalbumins. To determine the thermal stability of the Mg(II) form of parvalbumin, the intensities of several ^{1}H NMR resonances in its spectrum were monitored as a function of temperature. Two partially overlapping Phe ortho proton resonances centered at 7.65 ppm, the *N*-acetyl resonance at 2.04 ppm, two unassigned Met ϵ-CH_3 resonances at 1.97 and 1.96 ppm, and the doublet resonance of the γ-2 methyl of Val-106 at −0.35 ppm were analyzed and their average areas plotted vs. temperature. As shown in Figure 6B, the T_M for this metal-bound form was estimated as 67 °C. The reductions in the negative ellipticities of the 222-, 262-, and 269-nm CD bands (Figures 6A and 7B) also demonstrated the increased stability of Mg(II)–parvalbumin relative to its apo form. However, the T_M for the Mg(II) form, as determined from the 222-nm band reduction,

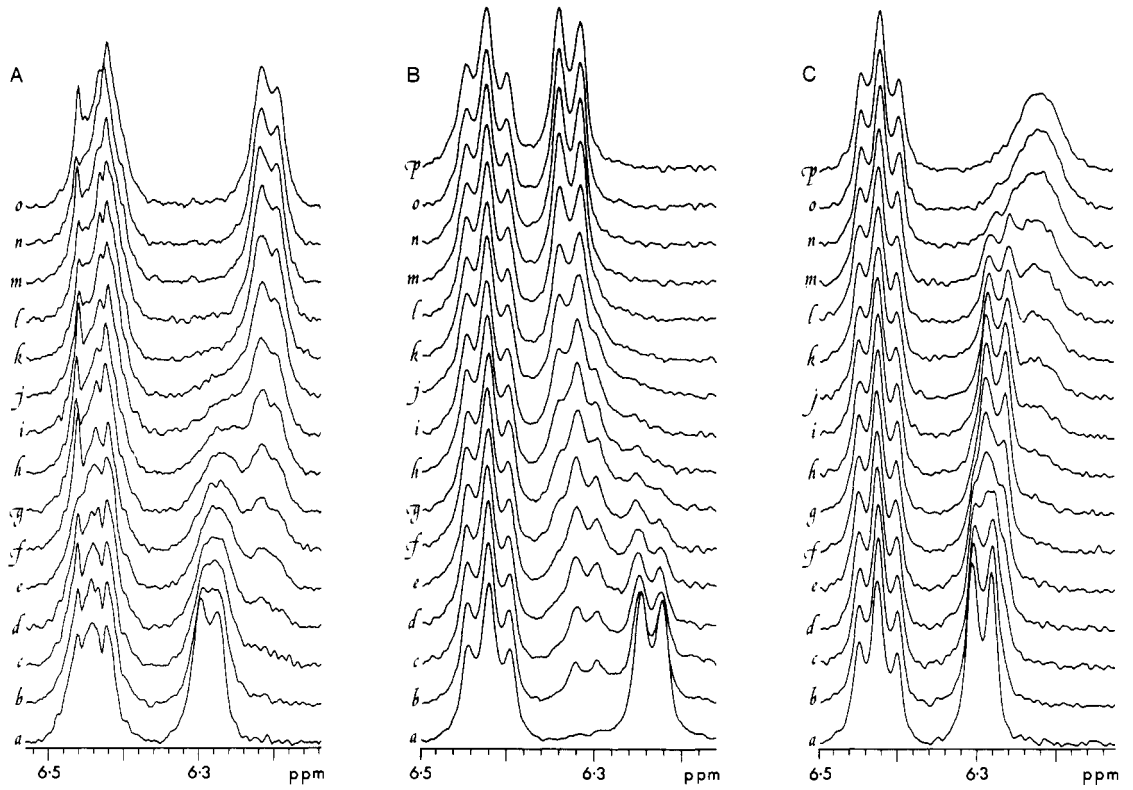

FIGURE 8: Partial aromatic region (6.5–6.2 ppm) of the ^{1}H NMR spectrum of rat parvalbumin: changes induced by metal ion binding. (A) Mg(II) titration of rat apo-α-parvalbumin; (B) Ca(II) titration of Mg(II)–parvalbumin; (C) Lu(III) titration of Ca(II)–parvalbumin. Selected metal:parvalbumin ratios for the spectra above are as follows: (A) a = 0.000, g = 1.085, l = 1.990, and o = 2.895; (B) a = 0.000, f = 0.970, l = 1.940, and p = 2.587; (C) a = 0.000, e = 0.495, i = 0.990, l = 1.414, and p = 2.404. The doublet resonance that underwent change during each titration has been assigned to the ortho protons of Phe-47; the triplet resonance that was not affected has been assigned tentatively to the meta protons of Phe-29. See text for titration conditions.

was 54 °C, considerably less than the NMR-determined T_M. The origin of this difference in T_M's is uncertain; however, due to the method of preparation of rat apo-α-parvalbumin, the concentration of KCl in the NMR sample may have been twice that of the CD sample. A higher salt concentration may have stabilized the Mg(II)–protein in the NMR sample (Filimonov et al., 1978), although it is unclear why the apo form was not also affected.

As for Ca(II)–parvalbumin, neither the reductions in ^{1}H NMR resonance intensities (Figure 6B) nor the reductions in CD band ellipticities (Figures 6A and 7C) were significant up to 60 °C. Heating to 85 °C allowed the NMR-deduced T_M to be estimated as 87 ± 2 °C; extrapolation of the 222-nm curve in Figure 6A suggested that the CD-deduced T_M was the same. These estimates of the melting temperature of the Ca(II) form of rat α-parvalbumin are quite similar to the T_M = 90 °C for carp pI = 4.25 parvalbumin determined from microcalorimetric measurements (Filimonov et al., 1978).

Metal Ion Chelation Studies. Parvalbumins form stable complexes simultaneously with 2 equiv of divalent or trivalent metal ions. Therefore, titration of one homogeneous form of the protein will generate a maximum of four distinguishable parvalbumin complexes: the unreacted initial form, in which both sites are either unoccupied or filled with the same type of metal ion; the final form, in which both sites are occuppied by the titrant metal ion; two intermediate heterogeneous forms, in which one *or* the other site is filled by the titrant metal ion. If the chemical shifts of the ^{1}H NMR resonances of each form differ from those of the others *and* if the exchange among these forms is slow on the NMR time scale, four sets of ^{1}H NMR resonances, one corresponding to each of the four metal ion–parvalbumin complexes, will be observed. The four overall stability constants β that define the equilibria among these forms will therefore determine the distribution of parvalbumin among its four coexisting species. However, if one assumes that the inherent complex stability of each site is *not* significantly altered by the complexation state of the other, then *two* β's are sufficient to describe the distribution of species.

(A) Mg(II) Titration. As already mentioned, the changes induced in the ^{1}H NMR spectrum of rat apo-α-parvalbumin by Mg(II) binding were slight. Most were subtle, poorly resolved, and therefore of little use in determining parvalbumin's affinity for Mg(II) ions. However, a few were clear enough to define the progressive slow-exchange conversion of the apo form to the Mg(II)-bound form. Shown in Figure 8A is the Mg(II)-induced shift of the ortho proton Phe-47 doublet resonance of the apo form (6.29 ppm) to a position slightly upfield in the Mg(II) form (6.20 ppm). The apo doublet resonance appeared to broaden slightly as it decreased in intensity, an indication that exchange between the apo and Mg(II)-bound forms of parvalbumin was not fully in the limit of slow exchange, the resonances of intermediate monosubstituted Mg(II) forms being only marginally different from either the apo or fully loaded Mg(II) forms. Two sets of variable-line-width Gaussian curves were used to simulate the line shapes of these Phe-47 resonances, yielding the relative proportions of initial and final forms. Plotted as a function of the Mg(II):parvalbumin ratio (Figure 10A), the fractional area of the 6.29 ppm resonance declined in a nonlinear fashion, being curved slightly upward relative to a truly linear decrease from 0 → 2 Mg(II):parvalbumin. Because the resonance intensity at 6.20 ppm represented the balance of the normalized intensity of these ortho proton Phe-47 resonances, its nonlinear increase from 0 → 2 Mg(II):parvalbumin was necessarily curved slightly downward. In a similar manner, the resonance areas of the His-48 C_2H singlet (not shown) were determined.

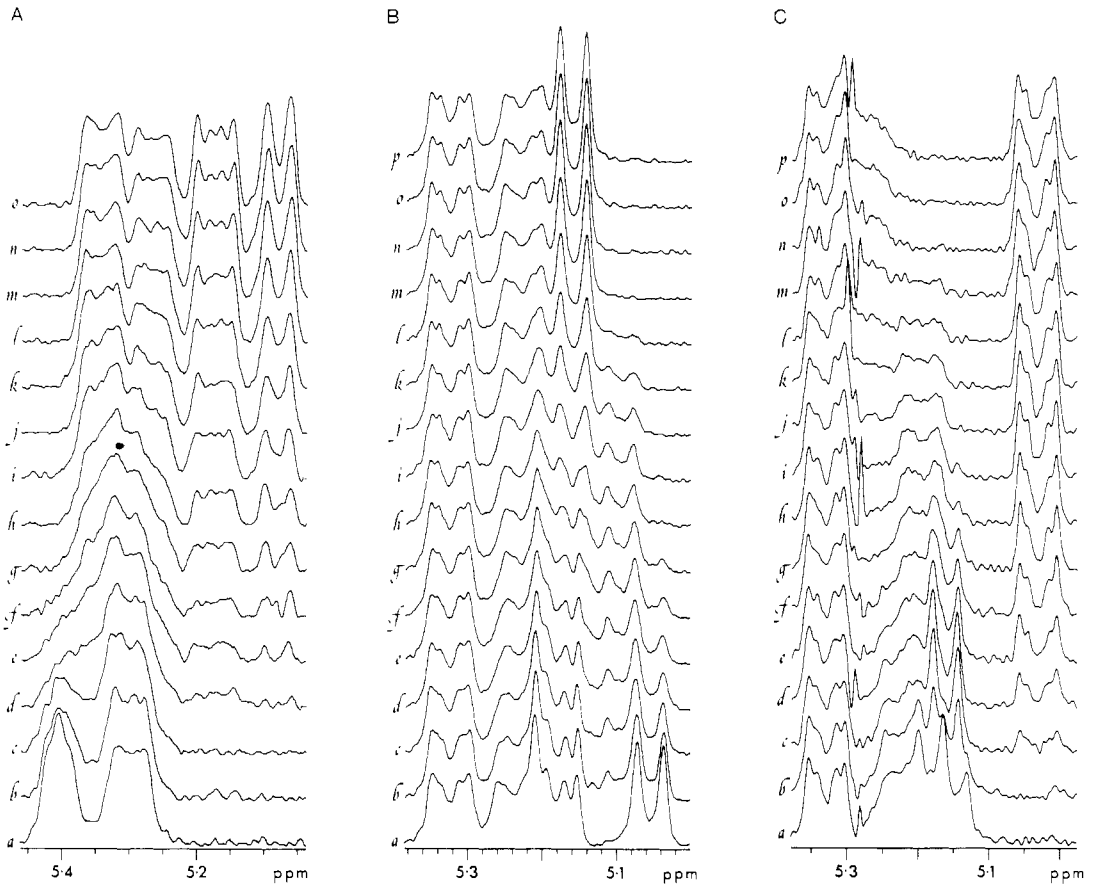

FIGURE 9: Downfield-shifted α-CH region (5.5–5.0 ppm) of the ^{1}H NMR spectrum of rat parvalbumin: changes induced by metal ion binding. (A) Mg(II) titration of rat apo-α-parvalbumin; (B) Ca(II) titration of Mg(II)–parvalbumin; (C) Lu(III) titration of Ca(II)–parvalbumin. Selected metal:protein ratios are listed in the legend of Figure 8. See text for titration conditions.

The decrease in the area of the initial resonance at 7.792 ppm and the complementary increase in the area of the resonance at 7.748 ppm were also quite nonlinear. The two α-CH resonances at 5.173 and 5.079 ppm (Figure 9A) followed increases similar to that described for the 6.20 ppm resonance of Phe-47 (Figure 8A). The four distribution profiles in Figure 10A indicated not only that Mg(II) binds to the two sites of rat apo-α-parvalbumin independently but also that the stabilities of the Mg(II) complexes at the two sites are slightly different. Having attributed the observed resonance decreases and increases to single complexes or sums of complexes as defined in Figure 10A, we determined the Mg(II) stability constants for parvalbumin's two sites to be $\beta_{Mg:1} = 5.6 \times 10^4$ M^{-1} and $\beta_{Mg:2} = 8.3 \times 10^4 M^{-1}$. Because of Phe-47's apparently greater sensitivity to metal ion exchange at the CD site (see Lu(III) Titration), we tentatively concluded that $\beta_{Mg:CD} = \beta_{Mg:1}$ and $\beta_{Mg:EF} = \beta_{Mg:2}$ (Table I).

(B) Ca(II) Titration. Figures 8B and 9B illustrate the analogous Ca(II)-induced changes in the spectrum of Mg(II)–parvalbumin. The triplet resonance at 6.42 ppm (tentatively assigned to the meta protons of Phe-29; Williams et al., 1986) remained unchanged during the Mg(II) → Ca(II) exchange reaction (Figure 8B). The ortho Phe-47 resonance (6.24 ppm) of the Mg(II) form decreased in intensity upon Ca(II) addition without signs of exchange broadening. Unlike the Mg(II) titration of rat apo-α-parvalbumin, formation of intermediate mixed-metal Mg(II):Ca(II) species was clearly indicated. Just downfield of its initial position, a doublet resonance from an intermediate form (6.31 ppm) arose in characteristic slow-exchange fashion, decreasing after reaching its maximum intensity at a Ca(II):parvalbumin ratio of 1. The doublet ortho Phe-47 resonance of the fully loaded (Ca(II) form (6.33 ppm) progressively increased from the start of the titration, leveling off at a Ca(II):parvalbumin ratio of 2. A second intermediate doublet resonance was revealed from line-shape analyses of this series of Phe-47 resonances (Figures 10B and 11). Although the doublet of doublet resonances at 5.34 and 5.23 ppm were insensitive to exchange at either site, the doublet resonance at 5.05 ppm decreased in intensity from the onset of Ca(II) titration; a similar, though less-intense, doublet just downfield of its position in the Mg(II) form (5.10 ppm) grew to a maximum at a Ca(II):parvalbumin ratio of 1 before decreasing to zero near 2:1. The position of this resonance in the Ca(II) form was evidenced by the doublet at 5.17 ppm, which grew to a maximum near 2:1. The transitions from the Mg(II) form through intermediate Mg(II):Ca(II) forms to the final Ca(II) form were also observed for the broader, ε-CH_3 Met singlet resonance at 1.96 ppm (not shown). As was done previously for the Mg(II) titration of rat apo-α-parvalbumin, these Ca(II)-induced resonance intensity changes were plotted as a function of added Ca(II) (Figure 10B). Relative to the Mg(II) form, the stability constants for Ca(II)–parvalbumin were $\beta_{Ca:1} = 4.0 \times 10^3$ and $\beta_{Ca:2} = 1.8 \times 10^3$. Because the more downfield-shifted of the two Mg(II):Ca(II) intermediate doublets reached a maximum

Table I: Overall Stability Constants (β) of Selected Metal Complexes of Rat Parvalbumin

	CD chelate		EF chelate	
metal	rel β	abs β[a]	rel β	abs β[a]
Mg(II)		5.6×10^4		8.3×10^4
Ca(II)	3.0×10^3	1.7×10^8	1.0×10^3	9.1×10^7
Lu(III)	1.2×10^2	2.0×10^{10}	2.5×10^3	2.3×10^{11}

[a] Units = M^{-1}.

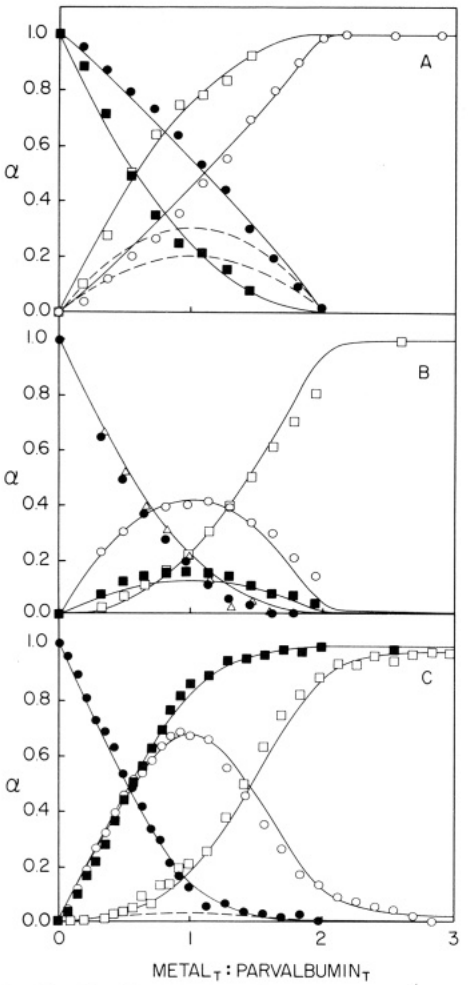

FIGURE 10: Species distribution of selected metal–parvalbumin complexes as determined by NMR-monitored metal ion titration studies (using the CD:EF notation to indicate the occuppancies at the metal sites). (A) Phe-47 doublet resonances at 6.29 (●; apo:apo plus apo:Mg) and 6.20 ppm (○; Mg:apo plus Mg:Mg); His-48 singlet resonances at 7.792 (■; apo:apo) and 7.748 ppm (□; Mg:apo plus apo:Mg plus Mg:Mg). (B) Phe-47 doublet resonances at 6.24 (●; Mg:Mg), 6.26 (■; Mg:Ca), 6.31 (○; Ca:Mg), and 6.33 ppm (□; Ca:Ca); α-CH doublet resonance at 5.05 ppm (△; Mg:Mg). (C) Phe-47 doublet resonances at 6.30 (●; Ca:Ca), 6.28 (○; Ca:Lu), and 6.23 ppm (□; Lu:Ca plus Lu:Lu); a Met ε-CH_3 singlet resonance at 1.93 ppm (■; Ca:Lu plus Lu:Lu).

intensity 2.2 times that of the other (Figure 10B), we concluded that the CD-site Mg(II) ion was preferentially displaced by Ca(II), assuming that the chemical shift of the ortho doublet of Phe-47 was more sensitive to CD-site exchange than it was to EF-site exchange [see Lu(III) Titration]. Therefore, the absolute values for the Ca(II) stability constants (i.e., the product of the relative $\beta \times \beta_{Mg}$ for each site) were determined to be $\beta_{Ca:CD} = 2.2 \times 10^8$ M^{-1} and $\beta_{Ca:EF} = 1.5 \times 10^3$ M^{-1} (Table I).

(*C*) *Lu(III) Titration.* Titration of the Ca(II) form of parvalbumin with Lu(III) also revealed a difference between the CD and EF sites as regards their metal ion preferences. Although the meta proton resonance of Phe-29 was, once again, insensitive to metal ion exchange as shown in Figure 8C, the ortho proton resonance of Phe-47 remained a useful probe of metal ion exchange: the initial doublet at 6.30 ppm steadily decreased in intensity as an intermediate doublet of nearly identical line width emerged at 6.28 ppm, reaching its maximum at 1:1 Lu(III):parvalbumin. Further upfield at 6.23 ppm appeared a much broader resonance with no distinct multiplet character; this resonance was attributed to the Phe-47

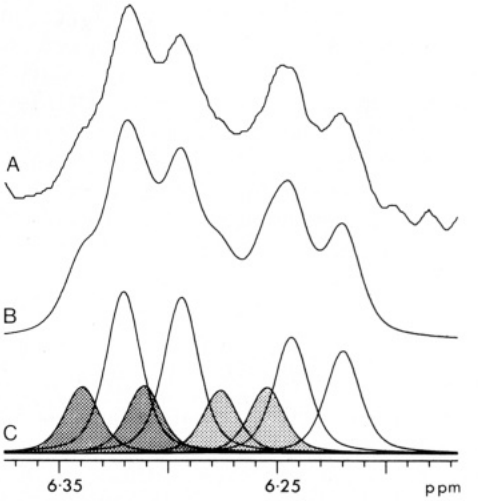

FIGURE 11: Curve analysis of the ortho doublet of Phe-47 during Ca(II) titration of the Mg(II) form of parvalbumin: (A) experimental spectrum at a Ca(II):parvalbumin ratio of 0.808 (same as trace e in Figure 9B); (B) calculated spectrum; (C) component doublet resonances of the calculated spectrum simulated by Gaussian line shapes in order to match the resolution-enhancement Gaussian function used to weight the FID spectrum. The doublet resonance of the Ca:Ca form is shaded dark gray; the doublet resonance of the Mg:Ca form [i.e., the form of parvalbumin with Ca(II) at the EF site] is shaded light gray. The larger unshaded doublet resonance arises from the Ca:Mg form; the smaller, from the Mg:Mg form.

ortho protons of the fully loaded Lu(III) form of parvalbumin, presumably broadened by slowed exchange between two orientations of the phenyl ring. The relative proportions of each form of the Phe-47 resonance were determined from line-shape analyses and plotted vs. added Lu(III). Curve fitting of these three data sets plus a fourth obtained from the changes observed for the broader Met ε-CH_3 singlet resonance at 1.93 ppm (not shown) yielded the following stability constants for the Lu(III)–parvalbumin complex relative to the Ca(III)–parvalbumin complex: $\beta_{Lu:1} = 1.2 \times 10^2$ and $\beta_{Lu:2} = 2.5 \times 10^3$. Because Lu(III) has been shown to preferentially displace Ca(II) from the EF site of p*I* = 4.25 carp parvalbumin (Corson et al., 1983a; Williams et al., 1984), we conclude that $\beta_{Lu:CD} = \beta_{Lu:1}$ and $\beta_{Lu:EF} = \beta_{Lu:2}$. The absolute values for the Lu(III) stability constants, derived from the β_{Ca}'s determined in this work, were $\beta_{Lu:CD} = 2.0 \times 10^{10}$ M^{-1} and $\beta_{Lu:EF} = 2.3 \times 10^{11}$ M^{-1} (Table I).

The Lu(III)-induced changes in the α-CH region of the spectrum are shown in Figure 9C. The continued *insensitivity* of the doublet of doublets resonance at 5.34 ppm to metal ion exchange was evident, as was the continued *sensitivity* of the resonance at 5.17 ppm. Note that in the initial spectrum of Figure 9C (trace a) this particular α-CH resonance appeared as a triplet whereas in the subsequent traces of Figure 9C and in the final spectrum of Figure 9B (trace p) it appeared as a doublet. We interpret the triplet pattern as an indication that scalar coupling to its adjacent nonexchanged NH was present initially whereas metal ion exchange and prolonged dissolution in D_2O facilitated its H → D exchange, reducing the multiplicity of this α-CH resonance from an apparent triplet to a doublet. This interpretation is consistent with our observation that the triplet resonance is also irreversibly transformed into a doublet resonance during pH titrations in D_2O (not shown). The slow rate of NH → ND exchange that this interpretation requires is also consistent with β-sheet H-bond formation between the metal-binding loops, the structural element from which these α-CH resonances presumably arise (Dalgarno et al., 1983). In addition, a new α-CH resonance at 5.04 ppm

arose with a profile of intensity increase similar to that of the broad Met ϵ-CH_3 resonance (Figure 10C); it was, therefore, attributed to the sum of the EF-exchanged Ca(II):Lu(III) intermediate form and the fully loaded Lu(III) form. Note the appearance of a broad, ill-defined resonance (relative area = 1) at 5.28 ppm (Figure 9C, trace p). This resonance, together with the broadened Phe-47 ortho doublet at 6.22 ppm and an unassigned broadened methyl resonance at 0.21 ppm (Figure 4C), may indicate that the residues in the cleft region between the CD and EF metal binding sites are less mobile, a conformational adjustment unique to the Lu(III) form of rat α-parvalbumin.

Discussion

When fully complexed with Ca(II), α- and β-parvalbumins are compact, highly organized structures: elements of both secondary and tertiary structure, well-defined in the crystalline form of one β-isoform (Kretsinger & Nockolds, 1973), appear undiminished in their solution conformations (Donato & Martin, 1974; Closset & Gerday, 1975; Birdsall et al., 1979; Lee & Sykes, 1983; Lee et al., 1985). When fully complexed with Mg(II), α- and β-parvalbumins retain most of the solution structure that characterizes their Ca(II) forms (Haiech et al., 1979; Birdsall et al., 1979; Moeschler et al., 1980), although the conformational differences between the Mg(II) and Ca(II) metal chelates have not yet been well-defined. When completely freed from metal, however, α-parvalbumins appear to differ significantly from β-parvalbumins: whereas the former possess much of both secondary and tertiary structure typical of their Ca(II) solution forms (Closset & Gerday, 1975, Gosselin-Rey & Gerday, 1977; Haiech et al., 1979), the later lack nearly all indications of an organized tertiary conformation (Parello et al., 1974; Closset & Gerday, 1975; Gosselin-Rey & Gerday, 1977; Haiech et al., 1979; Birdsall et al., 1979; Cox et al., 1979; Cavé et al., 1979; Permyakov et al., 1980; Seamon & Kretsinger, 1983). In an attempt to define precisely the metal(II)-induced changes in the conformation of the rat α-parvalbumin from skeletal muscle, we have examined in detail the solution structures of its apo, Mg(II), Ca(II), and Lu(III) forms using high-resolution ^{1}H NMR and CD spectroscopic methods. Although apo-parvalbumins presumably do *not* exist in physiological medium due to the saturating levels of Mg(II), determination of the solution structure of the apo form has permitted us to address more confidently the question of parvalbumin's function.

All of the spectroscopic evidence gathered here indicates that the preferred solution conformation of rat apo-α-parvalbumin is *nearly identical* with those of its metal-bound forms, in agreement with the previous studies of rat α-parvalbumins cited above. The tertiary structure of this form seems entirely intact, several ^{1}H NMR resonances from Phe-24, His-26, Phe-29, Phe-47, His-48, and Val-106 serving as specific monitors of the integrity of the hydrophobic core. Because the core itself is formed from precise hydrophobic interactions of parvalbumin's six helical segments, these secondary structural elements, too, must necessarily be present; the strong 222-nm band in the CD spectrum of the apo form clearly supports this assessment. The apparent percent α-helix, estimated by the method of Chen et al. (1974), with the experimental ellipticities at 210, 215, 220, and 225 nm, resulted in a value of 42% for the apo form at 25 °C (Table II). Thermal denaturation of the apo form appears to eliminate *all* characteristic tertiary structure as well as to reduce its apparent α-helical content to approximately 20%. In addition, the sharpness of the transition between its structured and disordered forms indicates that denaturation is highly cooperative. This unfolded form of the apo species is, in fact, quite similar to what has been observed with various spectroscopic techniques for the apo form of several β-parvalbumins (Donato & Martin, 1974; Cave et al., 1979). We suggest, therefore, that one of the apparent differences between the α- and β-parvalbumins is in their inherent thermal stabilities, the T_M of the β-lineage proteins presumably being <25 °C. Indications that ΔH_d varies over the 25–45 °C range is consistent with denaturation studies of other proteins. For example, the partial molar heat capacity, ΔC_p, for the thermal transition of β-lactoglobulin, −2.1 kcal·mol^{-1}·deg^{-1}, has been attributed to denaturation-induced exposure of hydrophobic side chains to the aqueous environment (Tanford, 1968). As relates to the denaturation of parvalbumin, exposure of the hydrophobic core might well account for the observed temperature dependence of ΔH_d.

Table II: Fractional Contributions of Secondary Structural Elements to the Solution Conformation of Rat Parvalbumin[a]

form	$[\theta]_{222}$	α-helix	β-form	random coil
apo	−13 568	0.42	0.18	0.41
Mg(II)	−14 783	0.50	0.17	0.33
Ca(II)	−16 004	0.54	0.23	0.23

[a] Calculated by the method of Chen et al. (1974).

Compared to the relatively low T_M of rat apo-α-parvalbumin (35 °C), the tremendously increased stabilities of the Mg(II)- and Ca(II)-bound forms of parvalbumins are less well understood. The transitions from structured to disordered forms not only occur at higher temperatures but are also less sharp for both the Mg(II) and Ca(II) complexes, being most gradual for the Ca(II) chelate; this suggests that denaturation may not be fully cooperative, alghough neither steps in the melting curves nor ^{1}H NMR resonances indicative of intermediate forms were observed. Indeed, Permyakov and Burstein (1984) have shown by phenylalanine fluorescence spectroscopy that thermal denaturation of the Mg(II) form of α-parvalbumin from pike proceeds via a two-step route, the larger conformational change coinciding with the higher temperature transition. Because the formation of metal ion complexes appears to affect most regions of the protein only slightly, we suggest that the denaturation reaction is catalyzed by charge–charge repulsions between anionic ligands in the CD and EF metal-binding loops, causing a disruption of interdomain contacts. In other words, the phenomenal stability of the tertiary structure of metal-bound parvalbumins arises primarily from a combination of interactions not directly affected by metal ligation: hydrophobic contacts between the *three* helix–loop–helix domains; ion pair bonds such as the internal Glu-81–Arg-75 salt bridge (Kretsinger & Nockolds, 1973); a network of paired surface charges such as the Lys-27–carboxy terminus ion pair (Corson et al., 1986). As long as the bound metal ions are able to effectively shield the electrostatic ligand–ligand repulsions, the protein conformation is stable; the formation of metal–ligand bonds, therefore, serves the dual function of eliminating the destabilizing effect of clustered negative charges while at the same time contributing to the overall stability through additional ion pair interactions. In this regard, it is interesting to note that the analogous high-affinity domains of troponin C and calmodulin (i.e., domains III and IV) melt as a single "cooperative block" in saturating levels of Ca(II) but as a two-domain substructure in the absence of divalent cations (Tsalkova & Privalov, 1985). By contrast, thermal denaturation of rat α-parvalbumin is apparently different, its apo form melting as a cooperative unit whereas its metal-bound forms showing signs of decreased cooperativity.

Although the Mg(II) titration of rat apo-α-parvalbumin failed to show any ^{1}H NMR resonances uniquely assignable to mono-Mg(II) complexes, the presence of these intermediate forms was verified from analyses of the species distribution profiles. For example, the crossover in the resonance intensities of the His-48 C_2H proton not only occurred at a Mg(II):parvalbumin ratio of only 0.6 but also indicated that the detected species were present in equal amounts. If intermediate species were *not* formed, then only fully apoparvalbumin or fully Me(II)-bound parvalbumin would be present. In this instance, even with an infinitely high Mg(II) affinity, the crossover at $\alpha = 0.5$ should not occur until the Mg(II):parvalbumin ratio reaches 1. As this is not the case, a mono-Mg(II) complex(es) must be formed. This inference is supported by the analysis of the nonlinear profiles of the Phe-47 ortho doublet resonance intensity changes, which suggests that the affinities for the two metal-binding sites are different, favoring slightly the formation of the EF-site Mg(II) complex.

Mg(II) → Ca(II) exchange also proceeds through intermediate forms. The direct observation of ^{1}H NMR resonances assignable to the intermediate Mg(II):Ca(II) mixed complexes showed that Ca(II) complex formation at one site is independent of exchange at the other. Furthermore, the CD-site Mg(II) ion is more labile to exchange than is EF-site Mg(II). In close aggreement with prevailing sentiment (Haiech et al., 1979; Moeschler et al., 1980), both Mg(II) and Ca(II) binding in parvalbumin are *noncooperative* processes, the CD and EF sites maintaining inherently different, although nearly equal, affinities for a given divalent metal ion.

As indicated in Table II, the CD spectra of the apo, Mg(II), and Ca(II) forms of rat α-parvalbumin can all be analyzed in terms of α-helix, β-form, and random-coil contributions to optical activity. However, because the apo and metal-bound forms are so exceedingly similar in both secondary *and* tertiary structure, we suggest that the small increases in negative ellipticity of the 222-nm CD band that accompany Mg(II) and Ca(II) chelation may arise from the asymmetric disposition of peptide carbonyls in the loops wrapped around the chelated metal ions (*configurational effect*) and/or transmission of asymmetry from the α-carbons to the carboxyl functions of the liganding Asp and Glu residues (*vicinal effect*) (Hawkins, 1971; Legrand & Rougier, 1977; Vallee & Holmquist, 1983).

Relative to the amino acid sequence of rat parvalbumin, the α-isoform from rabbit skeletal muscle is most homologous, containing only 14 substitutions (Barker et al., 1978). The Mg(II) and Ca(II) stability constants for rat parvalbumin determined in this work compare well with those published for the rabbit isoform: $\beta_{Mg} = 6.3 \times 10^4$ M^{-1} (Haiech et al., 1979) to 2.3×10^5 M^{-1} (Cox et al., 1977) and $\beta_{Ca} = 1.5 \times 10^8$ M^{-1} (Haiech et al., 1979) to 1.0×10^9 M^{-1} (Cox et al., 1977). In addition, although Lu(III) displaces Ca(II) easily from either site in rat α-parvalbumin, this lanthanide prefers complexation at the EF site by a factor of 22. Optical stopped-flow studies of the release of Yb(III) from 1:1 mixtures of ytterbium–parvalbumin indicate that this lanthanide is bound to the EF site in 4-fold excess, exactly as would be predicted by an EF-site affinity 22 times that of the CD site (D. C. Corson and B. D. Sykes, unpublished results). Similar exchange selectivity has been noted previously for other β-parvalbumins (Lee & Sykes, 1981; Corson et al., 1983a). The functional independence of metal ion chelation at the CD and EF sites, emphasized by Ca(II) → Ln(III) exchange, is a feature apparently common to most parvalbumins, regardless of lineage.

The highly specific line broadening of several ^{1}H NMR resonances in the spectrum of the Lu(III) form (6.20, 5.17, and 0.20 ppm) suggests that the mobilities of the side chains of Phe-47 and an unassigned isoleucine residue are reduced relative to the other forms of parvalbumin. In both the Mg(II) and Ca(II) complexes, the ortho doublet of Phe-47 is well resolved; in the Lu(III) form, however, the doublet character of this resonance is lost to exchange broadening. Likewise, the triplet resonance at 0.3 ppm in the Mg(II) form is severely broadened in the Lu(III) form [note: in the Ca(II) form this resonance has already lost most of its triplet character, presumably a result of exchange broadening even in this complex]. The region affected appears to be localized near the position of Phe-47; the apparent compression may, therefore, be limited to the contacts helix C and the CD loop make with the EF domain. If this is the case, Ile-49 (also in helix C) or Ile-58 (in the CD binding loop) may be one of the affected residues, leading to a tentative assignment of the resonance at 0.2 ppm in the spectrum of Ca(II)–parvalbumin.

Conclusions

Even in the absence of metal(II) ion, parvalbumin is capable of assuming a comformation in solution that is exceedingly similar to its native metal-bound forms. Its potential as a metal ion chelator is, therefore, tremendously enhanced, the liganding carboxyls being extremely limited in translational freedom. A more or less rigid structure of the preformed parvalbumin is consistent with its proposed function as a Ca(II) buffer. Large changes in conformation are *neither required* to chelate free Ca(II) *nor induced* by Ca(II) chelation.

Acknowledgments

We thank M. Natriss for analyses of the amino acid samples, Dr. R. Audette for atomic absorption analyses of $CaCl_2$, $MgCl_2$, and rat apo-α-parvalbumin solutions, and Dr. R. Jordan for a helpful discussion of cryptates.

Registry No. Mg, 7439-95-4; Ca, 7440-70-2; Lu, 7439-94-3.

References

Barker, W. C., Ketcham, L. K., & Dayhoff, M. D. (1978) in *Atlas of Protein Sequence and Structure* (Dayhoff, M. D., Ed.) pp 273–283, National Biomedical Research Foundation, Washington, DC.

Beck, M. T. (1970) in *Chemistry of Complex Equilibria* (Chalmers, R. A., Transl. Ed.) Chapter 11, Van Nostrand-Reinhold, London.

Berchtold, M. W., Heizmann, C. W., & Wilson, K. J. (1982) *Eur. J. Biochem. 127*, 381–389.

Birdsall, W. J., Levine, B. A., Williams, R. J. P., Demaille, J. G., Haiech, J., & Pechère, J.-F. (1979) *Biochimie 61*, 741–750.

Bose, K., & Bothner-By, A. A. (1983) *Biochemistry 22*, 1342–1347.

Cavé, A., Pages, M., Morin, P., & Dobson, C. M. (1979) *Biochimie 61*, 607–613.

Chen, Y. H., Yang, J. T., & Martinez, H. M. (1974) *Biochemistry 13*, 3350–3359.

Closset, J., & Gerday, C. (1975) *Biochim. Biophys. Acta 405*, 228–235.

Corson, D. C., Lee, L., McQuaid, G. A., & Sykes, B. D. (1983a) *Can. J. Biochem. Cell Biol. 61*, 860–867.

Corson, D. C., Williams, T. C., & Sykes, B. D. (1983b) *Biochemistry 22*, 5882–5889.

Corson, D. C., Williams, T. C., Kay, L. E., & Sykes, B. D. (1986) *Biochemistry* (first paper of three in this issue).

Cotton, F. A., & Harris, F. E. (1956) *J. Phys. Chem. 60*, 1451.
Cox, J. A., Wnuk, W., & Stein, E. (1977) in *Calcium-Binding Proteins and Calcium Function* (Wasserman, R. H., Corradino, R. A., Carafoli, E., Kretsinger, R. H., Maclennan, D. H., & Siefel, F. L., Eds.) pp 302–303, Elsevier, New York.
Cox, J. A., Winge, D. R., & Stein, E. A. (1979) *Biochimie 61*, 601–605.
Dalgarno, D., Levine, B. A., & Williams, R. J. P. (1983) *Biosci. Rep. 3*, 443–452.
Donato, H., & Martin, R. B. (1974) *Biochemistry 13*, 4575–4579.
Filimonov, V. V., Pfeil, W., Tsalkova, T. N., & Privalov, P. (1978) *Biophys. Chem. 8*, 117–122.
Gariêpy, J., Sykes, B. D., Reid, R., & Hodges, R. S. (1982) *Biochemistry 21*, 1506–1512.
Gariêpy, J., Sykes, B. D., & Hodges, R. S. (1983) *Biochemistry 22*, 1765–1772.
Gosselin-Rey, C., & Gerday, C. (1977) *Biochim. Biophys. Acta 492*, 53–63.
Haiech, J., Derancourt, J., Pechère, J.-F., & Demaille, J. G. (1979) *Biochemistry 18*, 2752–2758.
Haiech, J., Klee, C. B., & Demaille, J. G. (1981) *Biochemistry 20*, 3890–3897.
Hawkins, C. J. (1971) in *Absolute Configuration of Metal Complexes*, Chapter 5, Wiley-Interscience, New York.
IUPAC Commission on Equilibrium Data (1979) *IUPAC Chem. Data Ser. No. 22* (Part B).
IUPAC–IUB Joint Commission on Biochemical Nomenclature (1985) *J. Biol. Chem. 260*, 14–42.
Kretsinger, R. H., & Nockolds, C. E. (1973) *J. Biol. Chem. 248*, 3313–3326.
Leavis, P. C., Drabikowski, W. Rosenfeld, S., Grabarek, Z., & Geregly, J. (1977) in *Calcium-Binding Proteins and Calcium Function* (Wasserman, R. H., Corradino, R. A., Carafoli, E., Kretsinger, R. H., MacLennan, D. H., & Siegel, F. L., Eds.) pp 281–283, North-Holland, New York.
Lee, L., & Sykes, B. D. (1981) *Biochemistry 20*, 1156–1162.
Lee, L., & Sykes, B. D. (1983) *Biochemistry 22*, 4366–4373.
Lee, L., Corson, D. C., & Sykes, B. D. (1985) *Biophys. J. 47*, 139–142.
Legrand, M., & Rougier, M. J. (1977) in *Stereochemistry; Fundamentals and Methods* (Kagan, H. B., Ed.) Vol. 2, pp 103–155, Georg Thieme, Stuttgart.
Maximov, E. E., & Mitin, Y. V. (1979) *Biochimie 61*, 751–754.
Moeschler, H. J., Schaer, J.-J., & Cox, J. A. (1980) *Eur. J. Biochem. 111*, 73–78.
Oikawa, K., Kay, C. M., & McCubbin, W. D. (1968) *Biochim. Biophys. Acta 168*, 164–167.
Parello, J., Cavê, A., Puigdomenech, P., Maury, C., Capony, J. P., & Pechère, J.-F. (1974) *Biochimie 56*, 61–76.
Pechère, J.-F., Derancourt, J., & Haiech, J. (1977) *FEBS Lett. 75*, 111–114.
Permyakov, E. A., & Burstein, E. A. (1984) *Biophys. Chem. 19*, 265–271.
Permyakov, E. A., Yarmolenko, V. V., Emelyanenko, V. I., Burstein, E. A., Closset, J., & Gerday, C. (1980) *Eur. J. Biochem. 109*, 307–315.
Potter, J. D., & Gergely, J. (1975) *J. Biol. Chem. 250*, 4628–4633.
Reid, R. E., Gariêpy, J., Saund, A. K., & Hodges, R. S. (1981) *J. Biol. Chem. 256*, 2742–2751.
Schwarzenbach, G. (1952) *Helv. Chim. Acta 35*, 2344
Seamon, K. B., & Kretsinger, R. H. (1983) *Met. Ions Biol. 6*, 1–51.
Tanford, C. (1968) *Adv. Protein Chem. 23*, 122–282.
Tsalkova, T. N., & Privalov, P. L. (1985) *J. Mol. Biol. 181*, 533–544.
Vallee, B. L., & Holmquist, B. (1983) *Adv. Inorg. Biochem. 2*, 27–74.
Williams, T. C., Corson, D. C., & Sykes, B. D. (1984) *J. Am. Chem. Soc. 106*, 5698–5702.
Williams, T. C., Corson, D. C., McCubbin, W., Oikawa, K., Kay, C. M., & Sykes, B. D. (1986) *Biochemistry* (second paper of three in this issue).